A distributed feedback control strategy for optimal reactive power flow with voltage constraints

Saverio Bolognani, Ruggero Carli, Guido Cavraro, and Sandro Zampieri

***Abstract*—We consider the problem of exploiting the microgenerators dispersed in the power distribution network in order to provide distributed reactive power compensation for power losses minimization and voltage support. The proposed strategy requires that all the intelligent agents, located at the microgenerator buses, measure their voltage and share these data with the other agents on a cyber layer. The agents then actuate the physical layer by adjusting the amount of reactive power injected into the grid, according to a feedback control law that descends from duality-based methods applied to the optimal reactive power flow problem subject to voltage constraints. Convergence of the algorithm to the configuration of minimum losses and feasible voltages is proved analytically for both a synchronous and an asynchronous version of the algorithm, where agents update their state independently one from the other. Simulations are provided in order to illustrate the algorithm behavior, and the innovative feedback nature of such strategy is discussed.**

I. Introduction

Recent technological advances, together with environmental and economic challenges, have been motivating the deployment of small power generators in the low voltage and medium voltage power distribution grid. The availability of a large number of these generators in the distribution grid can yield relevant benefits to the network operation, which go beyond the availability of clean, inexpensive electrical power. They can be used to provide a number of ancillary services that are of great interest for the management of the grid [1], [2].

We focus in particular on the problem of optimal reactive power compensation for power losses minimization and voltage support. In order to properly command the operation of these devices, the distribution network operator is required to solve an *optimal reactive power flow* (ORPF) problem. Powerful solvers have been designed for the ORPF problem, and advanced optimization techniques have been recently specialized for this task [3], [4]. However, these solvers assume that an accurate model of the grid is available, that all the grid buses are monitored, that loads announce their demand profiles in advance, and that generators and actuators can be dispatched on a day-ahead, hour-ahead, and real-time basis. For this reason, these solvers are in general offline and centralized, and they collect all the necessary field data, compute the optimal configuration, and dispatch the reactive power production at the generators.

These tools cannot be applied directly to the ORPF problem faced in microgrids and, more in general, in low/medium voltage power distribution networks. The main reasons are that not all the buses of the grid are monitored, individual loads are unlikely to announce they demand profile in advance, the availability of small size generators is hard to predict (being often correlated with the availability of renewable energy sources). Moreover, the grid parameters, and sometimes even the topology of the grid, are only partially known, and generators are expected to connect and disconnect, requiring an automatic reconfiguration of the grid control infrastructure (the so called *plug and play* approach).

Different strategies have been recently proposed in order to address these issues, ranging from purely local algorithms, in which each generator is operated according to its own measurements [2], to distributed approaches that do not require any central controller, but still require measurements at all the buses of the distribution grid [5]. Only recently, algorithms that are truly scalable in the number of generators and do not require the monitoring of all the buses of the grid, have been proposed for the problem of power loss minimization (with no voltage constraints) [6], [7]. While these algorithms have been designed by specializing classical nonlinear optimization algorithms to the ORPF problem, they can also be considered as *feedback* control strategies. Indeed, the key feature of these algorithms is that they require the alternation of measurement and actuation based on the measured data, and therefore they are inherently online algorithms. In particular, the reactive power injection of the generators is adjusted by these algorithms based on the phasorial voltage measurements that are performed at the buses where the generators are connected. The resulting closed loop system features a tight dynamic interconnection of the *physical layer* (the grid, the generators, the loads) with the *cyber layer* (where communication, computation, and decision happen). In this paper, we design a distributed feedback algorithm for the ORPF problem with voltage constraints, in which the goal is to minimize reactive power flows while ensuring that the voltage magnitude across the network is larger than a given threshold.

In Section III, a model for the cyber-physical system of a smart power distribution grid is provided. In Section IV, the optimal reactive power flow problem with voltage constraints is stated. An algorithm for its solution is derived in Section V, by using the tools of dual decomposition. A synchronous and an asynchronous version of the algorithm are presented in Section VI and Section VII, respectively. The convergence of both the proposed algorithms is studied in Section VIII. Some simulations are provided in Section IX, while Section X concludes the paper discussing some relevant features of the feedback nature of the proposed strategy.

S. Bolognani is with the Laboratory for Information and Decision Systems, Massachusetts Institute of Technology, Cambridge, MA 02139 USA. Email: saverio@mit.edu

G. Cavraro, R. Carli, and S. Zampieri are with the Department of Information Engineering, University of Padova, Italy. Email: {carlirug, guido.cavraro, zampi}@dei.unipd.it.

II. Mathematical preliminaries and notation

Let $\mathcal{G} = (\mathcal{V}, \mathcal{E}, \sigma, \tau)$ be a directed graph, where $\mathcal{V}$ is the set of nodes, $\mathcal{E}$ is the set of edges, and $\sigma, \tau : \mathcal{E} \to \mathcal{V}$ are two functions such that edge $e \in \mathcal{E}$ goes from the source node $\sigma(e)$ to the terminal node $\tau(e)$.

Given two nodes of the graph $h, k \in \mathcal{V}$, we define the path $\mathcal{P}_{hk} = (v_1, \ldots, v_\ell)$ as the sequence of nodes, without repetitions, such that

- $v_1 = h$
- $v_\ell = k$
- for each $i = 1, \ldots, \ell - 1$, the nodes v_i and v_{i+1} are connected by an edge.

In the rest of the paper we will often introduce complex-valued functions defined on the nodes and on the edges. These functions will also be intended as vectors in $\mathbb{C}^n$ (where $n = |\mathcal{V}|$) and $\mathbb{C}^{|\mathcal{E}|}$. Given a vector u, we denote by $\bar{u}$ its (element-wise) complex conjugate, and by u^T its transpose. We denote by $\Re(u)$ and by $\Im(u)$ the real and the imaginary part of u, respectively.

Let moreover $A \in \{0, \pm 1\}^{|\mathcal{E}| \times n}$ be the incidence matrix of the graph $\mathcal{G}$, defined via its elements

$$[A]_{ev} = \begin{cases} -1 & \text{if } v = \sigma(e) \\ 1 & \text{if } v = \tau(e) \\ 0 & \text{otherwise.} \end{cases}$$

If the graph $\mathcal{G}$ is connected (i.e. for every pair of nodes there is a path connecting them), then $\mathbf{1}$ is the only vector in the null space $\ker A$, $\mathbf{1}$ being the column vector of all ones. We define by $\mathbf{1}_v$ the vector whose value is 1 in position v, and 0 everywhere else.

III. Cyber-physical model of a smart power distribution grid

In this work, we envision a *smart* power distribution network as a cyber-physical system, in which

- the **physical layer** consists of the power distribution infrastructure, including power lines, loads, microgenerators, and the point of connection to the transmission grid, while
- the **cyber layer** consists of intelligent agents, dispersed in the grid, and provided with actuation, sensing, communication, and computational capabilities.

A. Physical layer

For the purpose of this paper, we model the physical layer of a smart power distribution network as a directed graph $\mathcal{G}$, in which edges represent the power lines, and nodes represent the devices that are connected to the grid (see Figure 1, middle panel). These include loads, microgenerators, and also the point of connection to the transmission grid (called point of common coupling, or PCC, and indexed as node 0).

We limit our study to the steady state behavior of the system, when all voltages and currents are sinusoidal signals at the same frequency. Each signal can therefore be represented via a complex number $y = |y|e^{j\angle y}$ whose absolute value $|y|$ corresponds to the signal root-mean-square value, and whose phase $\angle y$ corresponds to the phase of the signal with respect to an arbitrary global reference.

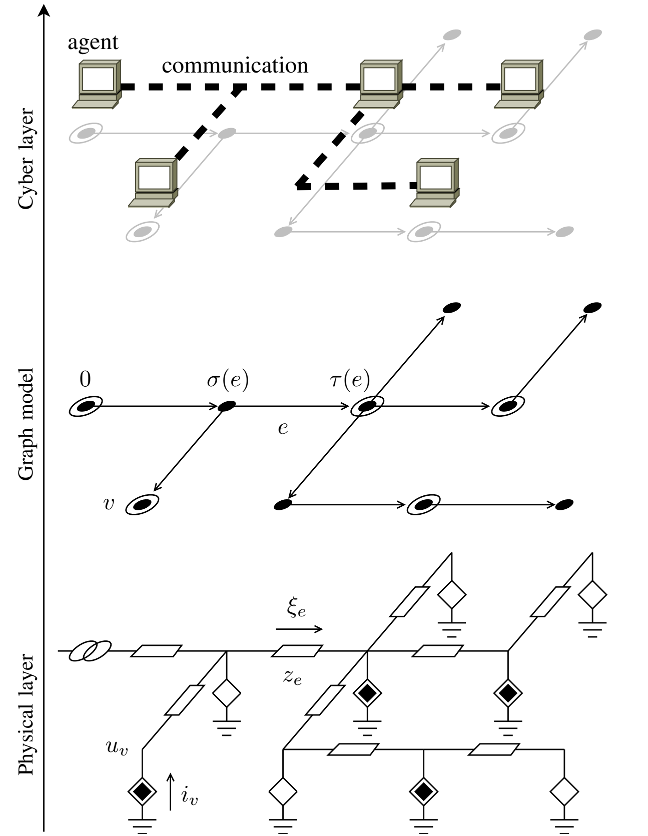

Figure 1. Schematic representation of the microgrid model. In the lower panel the physical layer is represented via a circuit representation, where black diamonds are microgenerators, white diamonds are loads, and the left-most element of the circuit represents the PCC. The middle panel illustrates the adopted graph representation for the same grid. Circled nodes represent both microgenerators and the PCC. The upper panel represents the cyber layer, where agents (i.e. microgenerator nodes and the PCC) are also connected via some communication infrastructure.

In this notation, the steady state of the grid is described by the following system variables (see Figure 1, lower panel):

- $u \in \mathbb{C}^n$, where u_v is the grid voltage at node v;
- $i \in \mathbb{C}^n$, where i_v is the current injected by node v;
- $\xi \in \mathbb{C}^{|\mathcal{E}|}$, where ξ_e is the current flowing on the edge e.

For every edge e of the graph, we define by z_e the impedance of the corresponding power line. We assume the following.

Assumption 1. *All power lines in the grid have the same inductance/resistance ratio, i.e.*

$$z_e = e^{j\theta}|z_e|$$

for any e in $\mathcal{E}$ and for a fixed θ.

This assumption is satisfied when the grid is relatively homogeneous, and is reasonable in most practical cases (see for example the IEEE standard testbeds [8]).

The following physical constraints are satisfied by u, i and

ξ

$$A^T\xi + i = 0, \qquad (1)$$

$$Au + e^{j\theta}Z\xi = 0, \qquad (2)$$

where A is the incidence matrix of $\mathcal{G}$, and $Z = \mathrm{diag}(|z_e|, e \in \mathcal{E})$ is the diagonal matrix of line impedances. Equation (1) corresponds to Kirchhoff's current law (KCL) at the nodes, while (2) describes the voltage drop on the edges of the graph. From (1) and (2) we can also obtain

$$i = e^{-j\theta}Lu \qquad (3)$$

where L is the weighted Laplacian of the graph $L := A^TZ^{-1}A$.

Each node v of the grid is also characterized by a law relating its injected current i_v with its voltage u_v. We model the PCC as an ideal sinusoidal voltage generator at the microgrid nominal voltage U_N with arbitrary, but fixed, angle ϕ

$$u_0 = U_N e^{j\phi}. \qquad (4)$$

In the power system analysis terminology, node 0 is then a *slack bus* with fixed voltage magnitude and angle.

We model loads and microgenerators (that is, every node v of the microgrid except the PCC) via the following law relating the voltage u_v and the current i_v

$$u_v\bar{i}_v = s_v, \quad \forall v \in \mathcal{V}\backslash\{0\}, \qquad (5)$$

where s_v is the injected *complex power*. The quantities

$$p_v := \Re(s_v) \quad \text{and} \quad q_v := \Im(s_v)$$

are denoted as *active* and *reactive* power, respectively. The complex powers s_v corresponding to grid loads are such that $\{p_v < 0\}$, meaning that positive active power is *supplied* to the devices. The complex powers corresponding to microgenerators, on the other hand, are such that $\{p_v \geq 0\}$, as positive active power is *injected* into the grid. In the power system analysis terminology, all nodes but the PCC are being modeled as *constant power* or *P-Q buses*. Microgenerators fit in this model, as they generally are commanded via a complex power reference and they can inject it independently from the voltage at their point of connection [9], [10].

B. Cyber layer

We assume that every microgenerator, and also the PCC, correspond to an *agent* in the cyber layer (see the upper panel of Figure 1). We denote by $\mathcal{C}$ (with $|\mathcal{C}| = m$) this subset of the nodes of $\mathcal{G}$.

Each agent is provided with some computational capability, and with some sensing capability, in the form of a phasor measurement unit (i.e. a sensor that can measure voltage amplitude and angle [11]). Agents that corresponds to a microgenerator can also actuate the system, by commanding the amount of reactive power injected by that microgenerator (see Figure 2).

Finally, agents can communicate, via some communication channel that could possibly be the same power lines (via power line communication – PLC – technology). Motivated by this possibility, we define the neighbors in the cyber layer in the following way.

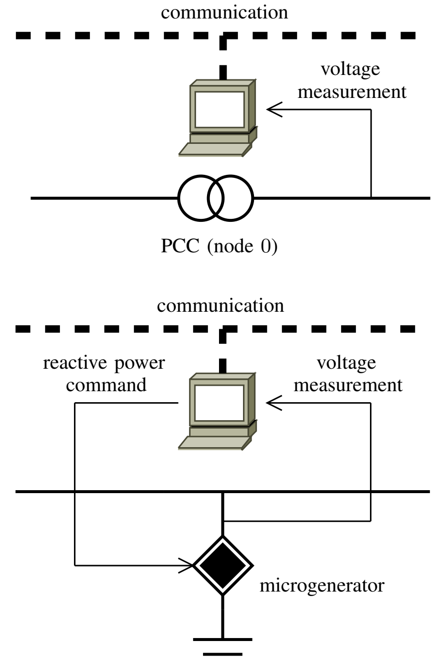

Figure 2. A schematic representation of the agents' capabilities and of the way in which agents of the cyber layer interface with the physical layers. The first panel represent the agent corresponding to the PCC (node 0), which is provided with voltage measurement capabilities. The second panel represents all the other agents, corresponding to microgenerator nodes, which are instead provided with both measurement and actuation capabilities. All the agent can also communicate via some communication channel, and have some on-board computational power.

Definition 1 (Neighbors in the cyber layer)**.** *Let $h \in \mathcal{C}$ be an agent of the cyber layer. The set of agents that are neighbors of h in the cyber layer, denoted as $\mathcal{N}(h)$, is the subset of $\mathcal{C}$ defined as*

$$\mathcal{N}(h) = \{k \in \mathcal{C} \mid \forall \mathcal{P}_{hk}, \mathcal{P}_{hk} \cap \mathcal{C} = \{h, k\}\}.$$

Figure 3 gives an example of such set.

We assume that every agent $h \in \mathcal{C}$ knows its set of neighbors $\mathcal{N}(h)$, and can communicate with them. Notice that this architecture can be constructed by each agent in a distributed way, for example by exploiting the PLC channel (as suggested for example in [12]). This allows also a plug-and-play reconfiguration of such architecture when new agents are connected to the grid.

IV. Optimal reactive power flow problem

We consider the problem of commanding the reactive power injection of the microgenerators in order to minimize power distribution losses on the power lines and to guarantee that the voltage magnitude stays above a given threshold. The decision variables (or, equivalently, the inputs of the system) are therefore the reactive power commands $q_h, h \in \mathcal{C}\backslash\{0\}$.

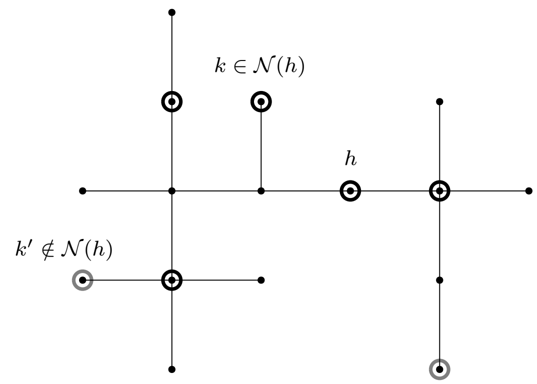

Figure 3. An example of neighbor agents in the cyber layer. Circled nodes (both gray and black) are agents (nodes in $\mathcal{C}$). Nodes circled in black belong to the set $\mathcal{N}(h) \subset \mathcal{C}$. Node circled in gray are agents which do not belong to the set of neighbors of h. For each agent $k \in \mathcal{N}(h)$, the path that connects h to k does not include any other agent besides h and k themselves.

Power distribution losses can be expressed, by using (2), as

$$J_{\text{losses}} := \sum_{e \in \mathcal{E}} |\xi_e|^2 \Re(z_e) = \bar{u}^T L u. \tag{6}$$

Given a lower bound $U_{\min}$ for the voltage magnitudes, we can therefore formulate the following optimization problem,

$$\min_{q_h, h \in \mathcal{C}\backslash\{0\}} \quad \bar{u}^T L u \tag{7a}$$

$$\text{subject to} \quad |u_h| \geq U_{\min}, \quad \forall h \in \mathcal{C}\backslash\{0\} \tag{7b}$$

where voltages u are a function of the decision variables $q_h, h \in \mathcal{C}\backslash\{0\}$, via the implicit relation defined by the system of nonlinear equations (3), (4), and (5). While we are not considering upper bounds on the bus voltage magnitudes, in the form $|u_h| \leq U_{\max}$, it will be clear in the following that they could be easily incorporated with minor modifications of the algorithm, at the cost of a slightly more complex notation.

In order to adopt a compact notation for the system inputs, measured outputs, and state, we introduce the following block decomposition of the vector of voltages u

$$u = \begin{bmatrix} u_0 \\ u_G \\ u_L \end{bmatrix},$$

where u_0 is the voltage at the PCC, $u_G \in \mathbb{C}^{m-1}$ are the voltages at the microgenerators, and $u_L \in \mathbb{C}^{n-m}$ are the voltages at the loads.

Similarly, we also define $s_G = p_G + jq_G$ and $s_L = p_L + jq_L$.

From a system-wide prospective, the control problem that we are considering is therefore characterized by

- the input variables q_G,
- the measured output variables $\begin{bmatrix} u_0 \\ u_G \end{bmatrix}$,
- the unmeasured disturbances p_L, q_L, p_G.

Remark. *While the decision variables of the ORPF problem (i.e. the input variables q_G) do not include the reactive power provided to the distribution grid by the PCC (i.e. $q_0 = u_0\bar{i}_0$), this quantity will also change every time the reactive power injections of the generators are updated by the algorithm, because the inherent physical behavior of the slack bus (the PCC) ensures that equations* (3), (4) *and* (5) *are automatically satisfied at every time.*

V. Dual decomposition

In this section, in order to derive a control strategy to solve the ORPF problem, we apply the tool of dual decomposition to (7). While problem (7) might not be convex in general, we rely on the results presented in [13] which show that zero duality gap holds for the ORPF problems, under some conditions that are commonly verified in practice. Based on this result, we use an approximate explicit solution of the nonlinear equations (3), (4), and (5), to derive the a *dual ascent algorithm* [14] that can be implemented by the agents.

In order to present the approximate solution, we need the following technical lemma.

Lemma 1 (Lemma 1 in [15])**.** *Let L be the weighted Laplacian of $\mathcal{G}$. There exists a unique symmetric, positive semidefinite matrix $X \in \mathbb{R}^{n \times n}$ such that*

$$\begin{cases} XL = I - \mathbf{1}\mathbf{1}_0^T \\ X\mathbf{1}_0 = 0. \end{cases} \tag{8}$$

The matrix X depends only on the topology of the grid power lines and on their impedance (compare it with the definition of Green matrix in [16]).

The matrix X has some notable properties, including the fact that

$$X_{hh} \geq X_{hk} \geq 0 \quad h, k \in \mathcal{V}, \tag{9}$$

and the fact that

$$(\mathbf{1}_h - \mathbf{1}_k)^T X (\mathbf{1}_h - \mathbf{1}_k) = \left|Z_{hk}^{\text{eff}}\right|, \quad h, k \in \mathcal{V}, \tag{10}$$

where Z_{hk}^{eff} represents the *effective impedance* of the power lines between node h and k. Notice that, if the grid is radial (i.e. $\mathcal{G}$ is a tree) then Z_{hk}^{eff} is simply the impedance of the only path from node h to node k.

By adopting the same block decomposition as before, we have

$$X = \begin{bmatrix} 0 & 0 & 0 \\ 0 & M & N \\ 0 & N^T & Q \end{bmatrix}, \tag{11}$$

with $M \in \mathbb{R}^{(m-1)\times(m-1)}$, $N \in \mathbb{R}^{(m-1)\times(m-n)}$, and $Q \in \mathbb{R}^{(n-m)\times(n-m)}$.

The following proposition provides the approximate relation between the grid voltages and the power injections at the nodes.

Proposition 1. *Consider the physical model described by the set of nonlinear equations* (1), (2), (4), *and* (5). *Node voltages then satisfy*

$$\begin{bmatrix} u_0 \\ u_G \\ u_L \end{bmatrix} = e^{j\phi} \left(U_N \mathbf{1} + \frac{e^{j\theta}}{U_N} \begin{bmatrix} 0 & 0 & 0 \\ 0 & M & N \\ 0 & N^T & Q \end{bmatrix} \begin{bmatrix} 0 \\ \bar{s}_G \\ \bar{s}_L \end{bmatrix} \right) + o\left(\frac{1}{U_N}\right), \tag{12}$$

where the little-o notation means that $\lim_{U_N \to \infty} \frac{o(f(U_N))}{f(U_N)} = 0$.

Proof: The proposition descends directly from Proposition 1 in [15]. ∎

The quality of this approximation relies on having large nominal voltage U_N and relatively small currents injected by the inverters (or supplied to the loads). This assumption is verified in practice, and corresponds to correct design and operation of power distribution networks, where indeed the nominal voltage is chosen sufficiently large (subject to other functional constraints) in order to deliver electric power to the loads with relatively small power losses on the power lines. In [15], a brief discussion about how this approximation extends the DC power flow model [17, Chapter 3] to the lossy case, has been provided.

Given the approximate explicit expression for voltages u presented in Proposition 1, we proceed by specializing the dual-ascent algorithm to problem (7).

The Lagrangian of the problem (7) is

$$\mathcal{L}(q_G, \lambda) = \bar{u}^T L u + \lambda^T \left(b\mathbf{1} - v_G\right) \tag{13}$$

where λ is the Lagrangian multiplier (i.e., the dual variables of the problem), where $b = U_{\text{min}}^2 / U_N^2$, and where v_G are the normalized squared voltage magnitudes at the generators

$$v_G = \frac{\bar{u}_G \odot u_G}{U_N^2},$$

$\odot$ being the operator for element-wise multiplication. Notice that, in order to simplify the derivation of the algorithm, we squared and normalized the left and right hand side of the inequalities (7b), without this having any effect on the optimization problem. Again, u_G and v_G are implicit functions of the decision variables q_G, even if the dependence has been omitted in the notation.

A dual ascent algorithm consists in the iterative execution of the following alternated steps

1) minimization of the Lagrangian with respect to the primal variables q_G

$$q_G(t+1) = \arg\min_{q_G} \mathcal{L}(q_G(t), \lambda(t)), \tag{14}$$

2) dual gradient ascent step on the dual variables

$$\lambda(t+1) = \left[\lambda(t) + \gamma \frac{\partial \mathcal{L}(q_G(t+1), \lambda(t))}{\partial \lambda}\right]_+, \tag{15}$$

where the $[\cdot]_+$ operator corresponds to the projection on the positive orthant, and where γ is a suitable positive constant.

In order to derive an expression for the minimizer $q_G(t+1)$ in (14), we need the following lemma.

Lemma 2. *Consider the Lagrangian* $\mathcal{L}(q_G, \lambda)$ *defined in* (13). *The partial derivative with respect to the primal variables* q_G *is*

$$\frac{\partial \mathcal{L}(q_G, \lambda)}{\partial q_G} = \frac{2}{U_N^2} \left(M q_G + N q_L - \sin\theta M \lambda\right) + o\left(\frac{1}{U_N^2}\right).$$

Proof: From (13) we have that

$$\frac{\partial \mathcal{L}(q_G, \lambda)}{\partial q_G} = \frac{\partial \bar{u}^T L u}{\partial q_G} - \left(\frac{\partial v_G}{\partial q_G}\right)^T \lambda. \tag{16}$$

In order to derive $\frac{\partial \bar{u}^T L u}{\partial q_G}$, we introduce the orthogonal decomposition $u = (u' + j u'') e^{j(\phi+\theta)}$, with $u', u'' \in \mathbb{R}^n$. We then have that, via Proposition 1,

$$\begin{aligned} u' &= \Re\left(u e^{-j(\phi+\theta)}\right) \\ &= \cos\theta U_N \mathbf{1} + \frac{1}{U_N} \begin{bmatrix} 0 & 0 & 0 \\ 0 & M & N \\ 0 & N^T & Q \end{bmatrix} \begin{bmatrix} 0 \\ p_G \\ p_L \end{bmatrix} + o\left(\frac{1}{U_N}\right), \end{aligned}$$

and similarly

$$\begin{aligned} u'' &= \Im\left(u e^{-j(\phi+\theta)}\right) \\ &= -\sin\theta U_N \mathbf{1} - \frac{1}{U_N} \begin{bmatrix} 0 & 0 & 0 \\ 0 & M & N \\ 0 & N^T & Q \end{bmatrix} \begin{bmatrix} 0 \\ q_G \\ q_L \end{bmatrix} + o\left(\frac{1}{U_N}\right). \end{aligned}$$

By using the fact that $\bar{u}^T L u = u'^T L u' + u''^T L u''$, we have

$$\begin{aligned} \frac{\partial \bar{u}^T L u}{\partial q_G} &= 2\left(\frac{\partial u''}{\partial q_G}\right)^T L u'' + 2\left(\frac{\partial u'}{\partial q_G}\right)^T L u' \\ &= -2\left[\frac{1}{U_N}\begin{bmatrix} 0 & M & N \end{bmatrix} + o\left(\frac{1}{U_N}\right)\right] L u'' + o\left(\frac{1}{U_N^2}\right) \\ &= \frac{2}{U_N^2}\begin{bmatrix} 0 & M & N \end{bmatrix} L \begin{bmatrix} 0 & 0 & 0 \\ 0 & M & N \\ 0 & N^T & Q \end{bmatrix} \begin{bmatrix} 0 \\ q_G \\ q_L \end{bmatrix} + o\left(\frac{1}{U_N^2}\right) \\ &= \frac{2}{U_N^2}\left(M q_G + N q_L\right) + o\left(\frac{1}{U_N^2}\right), \end{aligned} \tag{17}$$

where we used the fact that $L\mathbf{1} = 0$ and that, by Lemma 1, $LX = I - \mathbf{1}_0 \mathbf{1}^T$.

The same approximate solution (12), via some algebraic manipulations, allows us to express v_G as

$$v_G = \mathbf{1} + \frac{2}{U_N^2} \Re\left(e^{j\theta} M \bar{s}_G + e^{j\theta} N \bar{s}_L\right) + o\left(\frac{1}{U_N^2}\right). \tag{18}$$

We therefore have that

$$\frac{\partial v_G}{\partial q_G} = \frac{2}{U_N^2} \sin\theta M + o\left(\frac{1}{U_N^2}\right), \tag{19}$$

and finally, from (16), (17), and (19),

$$\frac{\partial \mathcal{L}(q_G, \lambda)}{\partial q_G} = \frac{2}{U_N^2}\left(M q_G + N q_L - \sin\theta M \lambda\right) + o\left(\frac{1}{U_N^2}\right).$$

∎

Given Lemma 2, we propose the following update step for q_G to minimize the Lagrangian with respect to the primal variables

$$q_G(t+1) = q_G(t) + \sin\theta \lambda(t) - (q_G(t) + M^{-1} N q_L). \tag{20}$$

Indeed, by plugging (20) into the expression for the partial derivative of the Lagrangian with the respect to q_G, provided

in Lemma 2, we obtain

$$\begin{aligned}\frac{\partial \mathcal{L}(q_G(t+1),\lambda)}{\partial q_G} &= \\ &= \frac{2}{U_N^2}\left(Mq_G(t+1)+Nq_L-\sin\theta M\lambda(t)\right)+o\left(\frac{1}{U_N^2}\right) \\ &= o\left(\frac{1}{U_N^2}\right),\end{aligned} \tag{21}$$

which vanishes for large nominal voltage U_N.

In order to derive the dual ascent step for the Lagrangian (13), it is enough to evaluate $\frac{\partial \mathcal{L}}{\partial \lambda}$ to see that

$$\frac{\partial \mathcal{L}(q_G,\lambda)}{\partial \lambda} = b\mathbf{1} - v_G,$$

in accordance to the well known result in dual decomposition that the dual ascent direction is given by the constraint violation. The proposed dual ascent step will therefore simply be

$$\lambda(t+1) = \left[\lambda(t) + \gamma\left(b\mathbf{1} - v_G(t+1)\right)\right]_+, \tag{22}$$

for some suitable $\gamma > 0$, where we recall that v_G is defined element-wise as $v_h = |u_h|^2/U_N^2$.

Remark. *It is well known that the dual ascent method guarantees primal feasibility of the solution, but does not guarantee primal feasibility of each intermediate step. Therefore, in the scenario that we are considering, voltage constraints* (7b) *will not be satisfied at every time. This is however acceptable: voltage constraints can be intended as soft constraints, because they do not derive from physical constraints on the system (like Kirchhoff laws). It will be shown via simulations in Section IX how the constraint violation is actually quite limited, also in the case of time-varying loads.*

VI. Synchronous algorithm

In this section, we show how the agents can implement the primal and dual steps (20) and (22) derived in the previous section. We assume here that the agents are coordinated, i.e. they can update their state variables q_h and λ_h, $h \in \mathcal{C}\backslash\{0\}$, synchronously.

In order to derive the update law for the agents, we need to introduce the following matrix G.

Lemma 3. *There exists a unique symmetric matrix $G \in \mathbb{R}^{m\times m}$ such that*

$$\begin{cases}\begin{bmatrix}0 & 0\\ 0 & M\end{bmatrix} G = I - \mathbf{1}\mathbf{1}_0^T \\ G\mathbf{1} = 0.\end{cases}$$

Proof: The following symmetric matrix G satisfies the conditions.

$$G = \begin{bmatrix}\mathbf{1}^T M^{-1}\mathbf{1} & -\mathbf{1}^T M^{-1} \\ -M^{-1}\mathbf{1} & M^{-1}\end{bmatrix}. \tag{23}$$

The proof of uniqueness, that we omit here, follows exactly the same steps as in the proof of Lemma 1. ∎

The matrix G has also a remarkable sparsity pattern, as the following lemma states.

Lemma 4. *The matrix G has the sparsity pattern induced by the Definition 1 of neighbor agents in the cyber layer, i.e.*

$$G_{hk} \neq 0 \quad \Leftrightarrow \quad k \in \mathcal{N}(h).$$

The proof is provided in the Appendix A, where we also discuss how the elements of G can be estimated by the agents, given a local knowledge of the power grid topology and parameters.

We therefore propose the following synchronous algorithm.

Synchronous algorithm

Let all agents (except the PCC) store an auxiliary scalar variable λ_h. Let γ be a positive scalar parameter, and let θ be the impedance angle defined in Assumption 1. Let G_{hk} be the elements of the matrix G defined in Lemma 3. At every synchronous iteration of the algorithm, each agent $h \in \mathcal{C}\backslash\{0\}$ executes the following operations in order:

- gathers the voltage measurements
$$\{u_k = |u_k|\exp(j\angle u_k), k \in \mathcal{N}(h)\}$$
from its neighbors;
- updates the auxiliary variable λ_h as
$$\lambda_h \leftarrow \left[\lambda_h + \gamma\left(\frac{U_{\text{min}}^2}{U_N^2} - \frac{|u_h|^2}{U_N^2}\right)\right]_+; \tag{24}$$
- based on the new value of λ_h, updates the injected reactive power q_h as
$$\begin{aligned} q_h \leftarrow\ & q_h + \sin\theta\lambda_h \\ & + \sum_{k\in\mathcal{N}(h)} G_{hk}|u_h||u_k|\sin(\angle u_k - \angle u_h - \theta). \end{aligned} \tag{25}$$

It can be shown, by using Lemma 4 and via some algebraic manipulation, that the update (25) can be also rewritten as

$$q_G \leftarrow q_G(t) + \sin\theta\lambda(t) + \Im\left(e^{-j\theta}\begin{bmatrix}0 & \operatorname{diag}(\bar{u}_G)\end{bmatrix} G \begin{bmatrix}u_0\\ u_G\end{bmatrix}\right),$$

which, by using the expression for u provided by Proposition 1, is equal to

$$q_G \leftarrow q_G + \sin\theta\lambda - (q_G + M^{-1}Nq_L) + o\left(\frac{1}{U_N}\right).$$

Similarly to what has been done in (21), we have that after the update

$$\frac{\partial \mathcal{L}(q_G,\lambda)}{\partial q_G} = o\left(\frac{1}{U_N^2}\right),$$

and therefore the update minimized the Lagrangian with respect to the primal variables, up to a term that vanishes for large U_N.

It is important to notice that the proposed synchronous algorithm requires that the agents actuate the system at every iteration, by updating the amount of reactive power that the

agent command to the microgenerators. Only by doing so, the subsequent measurement of the voltages will be informative of the new state of the system. The resulting control strategy is thus a *feedback strategy* that necessarily requires the real-time interaction of the controller (the cyber layer) with the plant (the physical layer), as depicted in Figure 4. This tight interaction between the cyber layer and the physical layer is the fundamental feature of the proposed approach, and allows to drive the system towards the optimal configuration, which depends also on the reactive power demand of the loads, without collecting this information from them. In a sense, the algorithm is inferring this hidden information from the measurement performed on the system during its execution.

VII. Asynchronous algorithm

In order to avoid the burden of coordination among the agents, we also propose an asynchronous version of the algorithm, in which the agents corresponding to the microgenerators update their state (q_h, λ_h) independently one from the other, based on the information that they can measure and that they can gather from their neighbors.

We assume that each agent (except for the agent located at the PCC) is provided with an individual timer, by which it is triggered. Timers tick randomly, with exponentially, identically distributed waiting times.

Asynchronous algorithm

Let all agents (except the PCC) store an auxiliary scalar variable λ_h. Let γ be a positive scalar parameter, and let θ be the impedance angle defined in Assumption 1. Let G_{hk} be the elements of the matrix G defined in Lemma 3.

When agent $h \in \mathcal{C}\backslash\{0\}$ is triggered by its own timer, it performs the following actions in order:

- gathers the voltage measurements $\{u_k = |u_k|\exp(j\angle u_k), k \in \mathcal{N}(h)\}$ from its neighbors;
- updates the auxiliary variable λ_h as
$$\lambda_h \leftarrow \left[\lambda_h + \gamma\left(\frac{U_{\min}^2}{U_N^2} - \frac{|u_h|^2}{U_N^2}\right)\right]_+ ;$$
- based on the new value of λ_h, updates the injected reactive power q_h as
$$q_h \leftarrow q_h + \sin\theta\lambda_h + \sum_{k\in\mathcal{N}(h)} G_{hk}|u_h||u_k|\sin(\angle u_k - \angle u_h - \theta).$$

The update equations for the asynchronous algorithm are exactly the same of the synchronous case. Here, however, we update both the primal and the dual variable of the agents independently and asynchronously.

VIII. Convergence analysis

In this section, we study the convergence of both the synchronous algorithm proposed in Section VI and of the asynchronous algorithm proposed in Section VII. For the analysis of the stability of both of them, we adopt again the approximated model proposed in Proposition 1, and we neglect the infinitesimal terms.

Notice that, by neglecting the infinitesimal terms, both the voltages u and the squared voltage magnitudes v_G become affine functions of the decision variables q_G, and therefore the ORPF problem (7) becomes a convex quadratic problem with linear inequality constraints, for which strong duality holds.

Let us define

$$\hat{v}_G := \mathbf{1} + \frac{2}{U_N^2}\Re\left(e^{j\theta}M\bar{s}_G + e^{j\theta}N\bar{s}_L\right), \tag{26}$$

For the synchronous case we consider the update equations

$$\lambda(t+1) = \left[\lambda(t) + \gamma\left(b\mathbf{1} - \hat{v}_G(t)\right)\right]_+, \tag{27}$$

for the dual variables, and

$$q_G(t+1) = q_G(t) + \sin\theta\lambda(t+1) - (q_G(t) + M^{-1}Nq_L). \tag{28}$$

for the primal variables.

Notice that the equilibrium (q_G^*, λ^*) of (27)-(28) is characterized by

$$b\mathbf{1} - \hat{v}_G(t) \le 0 \quad \text{and} \quad \sin\theta\lambda^* - (q_G^* + M^{-1}Nq_L) = 0,$$

and therefore, via (18) and via Lemma 2, we have that

$$\frac{|u_h(q^*)|^2}{U_N^2} \ge b + o\left(\frac{1}{U_N^2}\right), \ \forall h$$

and

$$\frac{\partial\mathcal{L}(q_G^*, \lambda^*)}{\partial q_G^*} = o\left(\frac{1}{U_N^2}\right),$$

which correspond, up to infinitesimal terms, to the necessary conditions for the optimality of (q_G^*, λ^*) according to Uzawa's saddle point theorem [18].

The following convergence result holds.

Theorem 1 (Synchronous case)**.** *Consider the dynamic system described by the update equations* (27) *and* (28)*. The equilibrium* (q^*, λ^*) *is asymptotically stable if*

$$\gamma \le \frac{U_N^2}{\sin^2\theta(m-1)D},$$

where $m-1$ *is the number of microgenerators and* $D := \max_h |Z_{0h}^{\mathit{eff}}|$ *is the maximum electric distance of a microgenerator from the PCC.*

The proof is presented in Appendix B.

For the asynchronous case, on the other hand, we introduce the following assumption.

Assumption 2. *Let* $\{T_i^{(h)}\}$*,* $i \in \mathbb{N}$*, be the time instants in which the agent* h *is triggered by its own timer. We assume that the timer ticks with exponentially distributed waiting times, identically distributed for all the agents in* $\mathcal{C}\backslash\{0\}$*.*

Let us define the random sequence $h(t) \in \mathcal{C}\backslash\{0\}$ which tells which agent has been triggered at iteration t of the algorithm. Because of Assumption 2, the random process $h(t)$ is an i.i.d. uniform process on the alphabet $\mathcal{C}\backslash\{0\}$. We therefore consider the following update equations, in which only the component $h(t)$ of the vectors q_G and λ is updated at time t:

$$\begin{cases} \lambda_{h(t)}(t+1) = \left[\lambda_{h(t)}(t) + \gamma\mathbf{1}_{h(t)}^T\left(b\mathbf{1} - \hat{v}_G(t)\right)\right]_+ \\ \lambda_k(t+1) = \lambda_k(t+1) \quad \text{for all } k \ne h(t), \end{cases} \tag{29}$$

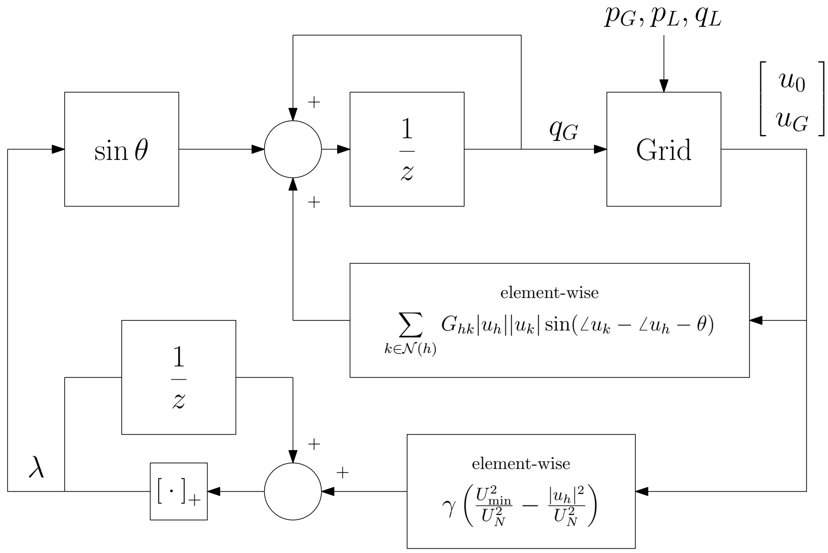

Figure 4. A block diagram representation of the synchronous control algorithm proposed in Section VI, where the tight interconnection of the cyber and the physical layer (i.e. the feedback strategy) is evident.

and

$$\begin{cases} q_{h(t)}(t+1) = q_{h(t)}(t) + \sin\theta\lambda_{h(t)}(t+1) \\ \qquad\qquad\qquad - \mathbf{1}_{h(t)}^T(q_G(t) + M^{-1}Nq_L), \\ q_k(t+1) = q_k(t) \quad \text{for all } k \neq h(t). \end{cases} \tag{30}$$

Notice that, also in the asynchronous case, Uzawa's necessary conditions for optimality are satisfied at the equilibrium of (29)-(30).

The following convergence result holds.

Theorem 2 (Asynchronous case)**.** *Consider the dynamic system described by the update equations* (29) *and* (30)*. Let Assumption 2 hold. Then the evolution $t \to (q(t), \lambda(t))$ converges almost surely to the equilibrium (q^*, λ^*) if*

$$\gamma \leq \frac{U_N^2}{\sin^2\theta(m-1)D},$$

where $m-1$ is the number of microgenerators and $D := \max_h |Z_{0h}^{\mathit{eff}}|$ is the maximum electric distance of a microgenerator from the PCC.

The proof is presented in Appendix B.

IX. Simulations

The algorithm has been tested on the testbed IEEE 37 [8], which is an actual portion of 4.8kV power distribution network located in California. The load buses are a blend of constant-power, constant-current, and constant-impedance loads, with a total power demand of almost 2 MW of active power and 1 MVAR of reactive power (see [8] for the testbed data). The length of the power lines range from a minimum of 25 meters to a maximum of almost 600 meters. The impedance of the power lines differs from edge to edge (for example, resistance ranges from 0.182 Ω/km to 1.305 Ω/km). However, the inductance/resistance ratio exhibits a smaller variation, ranging from $\angle z_e = 0.47$ to $\angle z_e = 0.59$. This justifies Assumption 1, in which we claimed that $\angle z_e$ can be considered constant across the network. We considered the scenario in which 5 microgenerators have been deployed in this portion of the power distribution grid (see Figure 5).

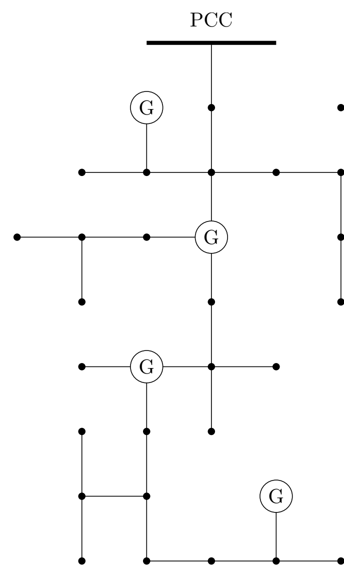

Figure 5. Schematic representation of the IEEE 37 test feeder [8], where 5 microgenerators have been deployed.

The lower bound for voltage magnitudes has been set to 96% of the nominal voltage. Both the synchronous and the asynchronous algorithm presented in Section VI and VII have been simulated on a nonlinear exact solver of the grid [19]. The approximate model presented in Proposition 1 has not been used in these simulations, being only a tool for the design of the algorithm and for the study of the algorithm's convergence. The parameter γ has been chosen as one half of the bound indicated by Theorem 1 and Theorem 2 for convergence. Timers in the asynchronous case have been tuned so that each agent is triggered, in expectation, at the same rate of the synchronous case.

A time-varying profile for the loads has been generated, in order to simulate the effect of slowly varying loads (e.g. the aggregate demand of a residential neighborhood), fast changing demands (e.g. some industrial loads), and intermittent large loads (e.g. heating).

The results of the simulation have been plotted in Figure 6. For both the synchronous and the asynchronous case, the power distribution losses and the lowest voltage magnitude measured by the microgenerators, are reported. The dashed line represents the case in which no reactive power compensation is performed. The thick black line represents the best possible strategy that solves the ORPF problem (7) (computed via a numerical centralized solver that have access to all the grid parameters and load data). The thin red line represents the behavior of the proposed algorithm.

It can be seen that the proposed algorithm achieves practically the same performance of the centralized solver, in terms of power distribution losses. Notice however that the proposed algorithm does not have access to the demands of the loads, which are unmonitored. The agents, located only at the microgenerators, can only access their voltage measurements and share them with their neighbors. Notice moreover that, as expected for duality based methods, the voltage constraint is satisfied only at the steady state. Therefore, in the time varying case simulated in this example, the voltage sometimes falls lightly below the prescribed threshold, when the power demand of the loads present abrupt changes. This effect is even more noticeable in the asynchronous case, where iteration times are not evenly spaced. It should be remarked, however, that the extent of this constraint violation depends on the rate at which the algorithms are executed, compared with the rate of variation of loads, and is ultimately a function of the communication resources that are available at the cyber level.

X. Conclusions

In this paper we proposed a distributed control law for optimal reactive power flow in a smart power distribution grid, based on a *feedback strategy*. Such a strategy requires the *interleaving of actuation and sensing*, and therefore the control action (the reactive power injections $q_h, h \in \mathcal{C}\backslash\{0\}$) is a function of the real time measurements (the voltages $u_h, h \in \mathcal{C}$). According to this interpretation, the active power injections in the grid ($p_h, h \in \mathcal{V}$) and the reactive power injection of the loads ($q_h, h \in \mathcal{V}\backslash\mathcal{C}$) can be considered as *disturbances* for the control system. As it happens in all feedback control systems, these quantities do not need to be known to the controller: in some sense, the agents are implicitly inferring this information from the voltage measurements performed on the grid. Similarly, it is also well known that the presence of feedback in the control action makes the closed loop behavior of the system less sensitive to model uncertainties. While we have not elaborated this point, we expect that the proposed strategy exhibits this kind of robustness. These features differentiate the proposed algorithm from most of the ORPF algorithms available in the power system literature, with the exception of some works, like [20], where however the feedback is only local, with no communication between the agents, and of [6] and [7]. Moreover, in the proposed feedback strategy, the controller (or optimizer) does not need to solve any model of the grid in order to find the optimal solution. While some knowledge of the grid parameters are used in the design and tuning of the algorithm, the online controller does not need to know or solve the nonlinear grid equations that are generally a critical issue in offline ORPF solvers. On the contrary, the computational effort required for the execution of the proposed algorithm is minimal. These features are extremely interesting for the scenario of low voltage or medium voltage power distribution networks, where real time measurement of the loads is usually not available, the grid parameters are partially unknown, and many buses are unmonitored.

While a feedback approach to the ORPF problem is quite a new contribution, similar methodologies have been used to solve other tasks in the operation of power grids (see Figure 7). In particular, in order to achieve realtime matching of the power demand and power generators, synchronous generators are generally provided with a local feedback control that adjusts the input mechanical power according to frequency measurements, in order to keep frequency sufficiently close to the desired nominal value (the primary frequency control in [21], see also [22], [23]). By adding a communication channel (a cyber layer) that enables coordination among the different agents, it is also possible to drive the system to the configuration of minimum generation costs [24]. Notice that, in this scenario, generators do not have access to the aggregate active power demand of the loads, but infer it from the purely local frequency measurements. This example share some qualitative similarities with the original approach presented in this paper, where agents do not have access to the individual or aggregated reactive power demand of the loads, but however can use voltage measurements to infer this information and, by coordinating their action, to drive the grid to the configuration of minimum losses.

As suggested in [25], a control-theoretic approach to the problem of optimal power flow enables also a number of analyses on the performance of the closed loop system that are generally overlooked when tackling the problem with the tools of nonlinear optimization. Examples are L_2-like metrics for the resulting losses in a time-varying scenario (see for example the preliminary results in [26]), robustness to measurement noise and parametric uncertainty, stability margin against communication delays. These analyses, still not investigated, are also of interest for the design of the cyber architecture that has to support this and other real time algorithms, because they can provide specifications for the communication channels, the communication protocols, and the computational resources that need to be deployed in a smart distribution grid.

Appendix A
G-parameters

Let us define the following parameters g_{hk}, $h, k \in \mathcal{C}$.

Definition 2 (g-parameters)**.** *For each pair $h, k \in \mathcal{C}$, let us*

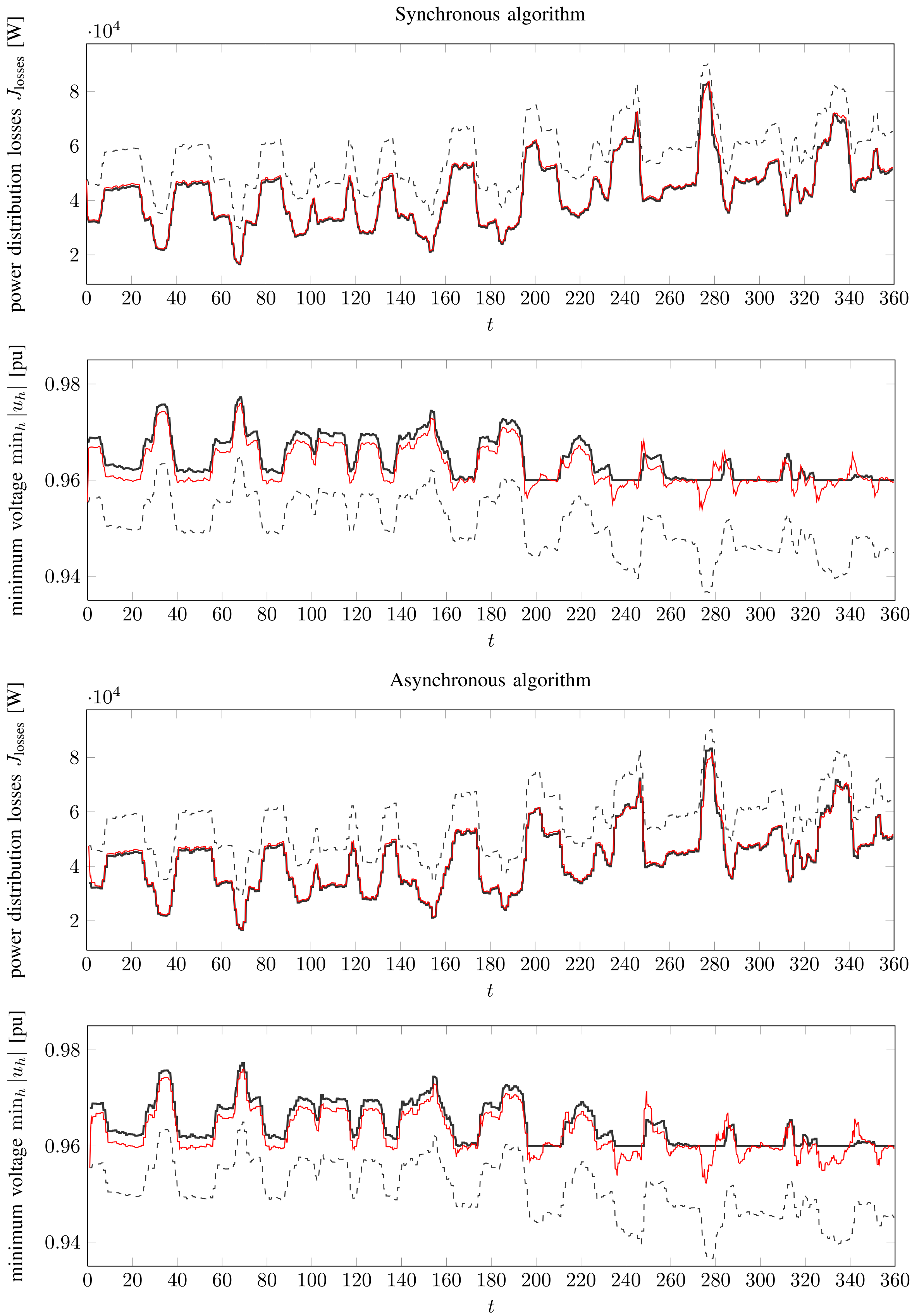

Figure 6. For both the synchronous and the asynchronous case, power distribution losses and the lowest measured voltages are plotted for the following cases: when no reactive power compensation is performed (dashed line), when an ideal centralized numerical controller commands the microgenerators (thick black line), and for the proposed algorithm, where microgenerators are commanded via a feedback law from the voltage measurements (thin red line).

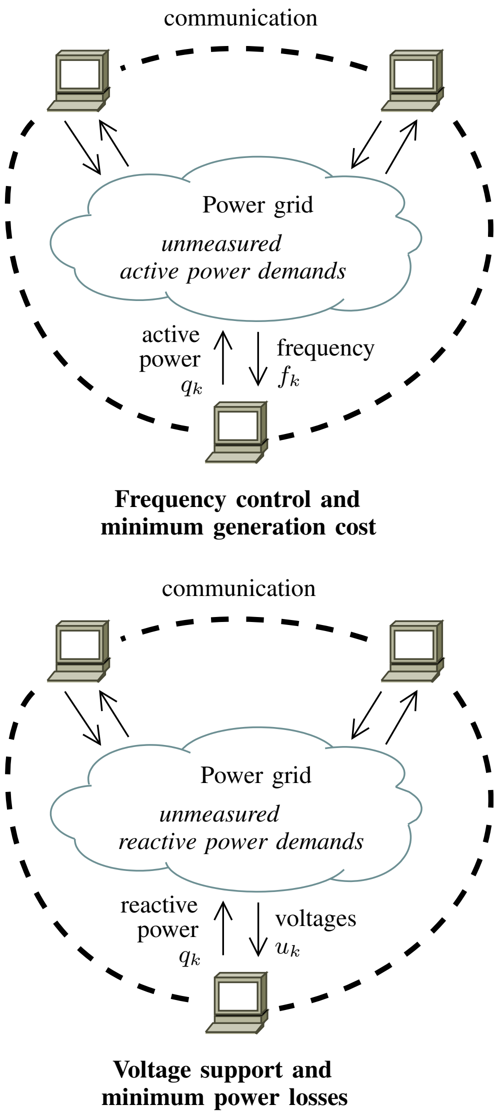

Figure 7. Qualitative comparison between primary frequency control in power grids (first panel) and the proposed feedback strategy for optimal reactive power flow (second panel).

define the parameter

$$g_{hk} = |i_h| \Bigg|_{\substack{u_k \;= 1 \\ u_\ell \;= 0,\ \ell \in \mathcal{C}\backslash\{k\} \\ i_\ell \;= 0,\ \ell \notin \mathcal{C}}} . \tag{31}$$

i.e. the current that would be injected at node h if

- *node k was replaced with a unitary voltage generator;*
- *all other nodes in $\mathcal{C}$ (the other agents) were replaced by short circuits;*
- *all nodes not in $\mathcal{C}$ (load buses) were replaced by open circuits.*

Notice that the parameters g_{hk} depend only on the grid electric topology, and that

$$g_{hk} \neq 0 \quad \text{if and only if} \quad k \in \mathcal{N}(h).$$

Figure 8 gives a representation of this definition. Notice that, in the special case in which the paths from h to its neighbors are all disjoint and unique paths, then $G_{hk} = (\sum_{e \in \mathcal{P}_{hk}} |z_e|)^{-1}$, i.e. the inverse of the impedance of the path connecting h to k.

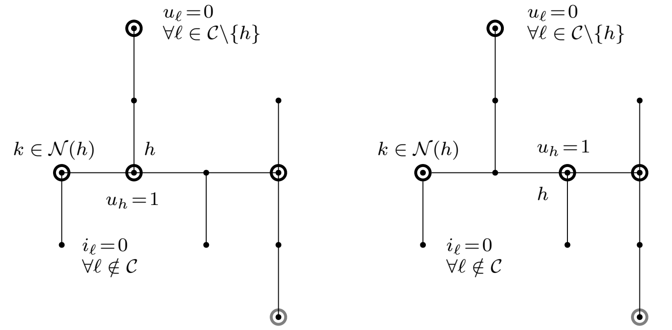

Figure 8. A representation of how the elements G_{kh} are defined. Notice that in the configuration of the left panel, as the paths from h to its neighbors $k \in \mathcal{N}(h)$ do not share any edge, the gains G_{kh} corresponds to the absolute value of the path admittances $1/|Z_{kh}|$.

As suggested in [12], these parameters can be estimated in an initialization phase via some ranging technologies over the PLC channel. Alternatively, this limited amount of knowledge of the grid topology can be stored in the agents at the deployment time. Finally, the same kind of information can be also inferred by specializing the procedures that use the extended capabilities of the generator power inverters for online grid sensing and impedance estimation [27], [28].

The following Lemma shows that the elements g_{hk} in Definition 2 correspond to the elements G_{hk} of the matrix G in Lemma 3.

Lemma 5. *Let G be the matrix defined in Lemma 3. Then, for all h, k, $G_{hk} = g_{hk}$ as defined in Definition 2.*

Proof: Let $\hat{G}$ be the matrix whose elements are the parameters g_{hk}. From Definition 2, we have that when $i_L = 0$,

$$\begin{bmatrix} i_0 \\ i_G \end{bmatrix} = \exp(-j\theta)\hat{G} \begin{bmatrix} u_0 \\ u_G \end{bmatrix}. \tag{32}$$

From circuit theory considerations, this implies that $\hat{G}\mathbf{1} = 0$. From (3) and by using the matrix X defined in Lemma 1, if $i_L = 0$, we have

$$\left(I - \mathbf{1}\mathbf{1}_0^T\right) \begin{bmatrix} u_0 \\ u_G \end{bmatrix} = e^{j\theta} \begin{bmatrix} 0 & 0 \\ 0 & M \end{bmatrix} \begin{bmatrix} i_0 \\ i_G \end{bmatrix}. \tag{33}$$

Therefore, by plugging (32) into (33), we have that $\left(I - \mathbf{1}\mathbf{1}_0^T\right) = \left[\begin{smallmatrix} 0 & 0 \\ 0 & M \end{smallmatrix}\right] \hat{G}$. ■

Appendix B
Proof of Theorems 1 and 2

We first introduce the following technical lemma.

Lemma 6. *Let M be the $(m-1) \times (m-1)$ block of X as defined in* (11)*. Let $\rho(M)$ be its spectral radius. Then*

$$\rho(M) \leq (m-1)D$$

where $D := \max_h |Z_{0h}^{\mathit{eff}}|$ is the maximum electric distance of a microgenerator from the PCC.

Proof: Because of (9), we have that $M_{hh} \geq M_{hk} \geq 0,\ \forall h, k$. Therefore

$$\begin{aligned}
\rho(M) &= \max_{\|\eta\|=1} \sqrt{\sum_h \left(\sum_k M_{hk}\eta_k\right)^2} \\
&\leq \max_{\|\eta\|=1} \sqrt{\sum_h \left(M_{hh}\sum_k \eta_k\right)^2} \\
&\leq \sqrt{\sum_h \left(M_{hh}\sqrt{m-1}\right)^2} \\
&\leq \sqrt{\sum_h \left(\max_h M_{hh}\sqrt{m-1}\right)^2} \\
&= \max_h M_{hh}(m-1).
\end{aligned}$$

By using the fact that, via (10), $M_{hh} = |Z_{0h}^{\text{eff}}|$, we prove the statement. ■

Proof of Theorem 1: Let (q_G^*, λ^*) be the equilibrium of the system (27)-(28), which satisfies the following equations

$$\sin\theta\lambda^* - (q_G^* + M^{-1}Nq_L) = 0 \tag{34a}$$
$$b - \hat{v}_h(q^*) \leq 0 \quad \forall h \in \mathcal{C} \tag{34b}$$
$$b - \hat{v}_h(q^*) < 0 \quad \Leftrightarrow \quad \lambda_h^* = 0.. \tag{34c}$$

We introduce the two following quantities

$$x(t) = q_G(t) - q_G^* \quad \text{and} \quad y(t) = \lambda(t) - \lambda^*.$$

The update for $x(t)$ is, given (28),

$$\begin{aligned}
x(t+1) &= q_G(t+1) - q^* \\
&= x(t) + \sin\theta\lambda(t+1) - (q_G(t) + M^{-1}Nq_L) \\
&\quad - \sin\theta\lambda^* + q_G^* + M^{-1}Nq_L \\
&= \sin\theta y(t+1),
\end{aligned}$$

where in the second step we used condition (34a).

We then consider the update equation for $y(t)$. From (27) we have

$$\begin{aligned}
&y(t+1) = \\
&\quad = \lambda(t+1) - \lambda^* \\
&\quad = [\lambda(t) + \gamma\,(b\mathbf{1} - \hat{v}(q(t)))]_+ - [\lambda^*] \\
&\quad = \left[y(t) + \lambda^* + \gamma\,(b\mathbf{1} - \hat{v}(q^*)) - \gamma\frac{2}{U_N^2}\sin\theta Mx(t)\right]_+ \\
&\qquad - [\lambda^*]_+\,,
\end{aligned}$$

where we used the fact that

$$\hat{v}(q(t)) = \hat{v}(q^*) + \frac{2}{U_N^2}\sin\theta Mx(t).$$

Let us define the constant vector

$$\alpha = \lambda^* + \gamma\,(b\mathbf{1} - \hat{v}(q_G^*))\,.$$

We then have, by using (34b) and (34c),

$$y(t+1) = \left[y(t) + \alpha - \gamma\frac{2}{U_N^2}\sin\theta Mx(t)\right]_+ - [\alpha]_+$$

which, by using the update equation for x, becomes

$$y(t+1) = \left[\left(I - \gamma\frac{2}{U_N^2}\sin^2\theta M\right)y(t) + \alpha\right]_+ - [\alpha]_+\,.$$

By using the fact that

$$\|a_+ - b_+\| \leq \|a - b\|,$$

we have that

$$\|y(t+1)\| \leq \left\|\left(I - \gamma\frac{2}{U_N^2}\sin^2\theta M\right)y(t)\right\|,$$

and therefore, as M is symmetric and positive definite, $y(t)$ converges to zero if

$$\gamma < \frac{U_N^2}{\sin^2\theta\rho(M)},$$

where $\rho(M)$ is the spectral radius of M.

By using Lemma 6, we then finally have the sufficient condition for convergence

$$\gamma < \frac{U_N^2}{\sin^2\theta(m-1)\max_h |Z_{0h}^{\text{eff}}|}.$$

■

Proof of Theorem 2: Consider the update equations (29) and (30) for the dual variables λ and for the primal variables q_G, respectively. Introducing the same variables y and x as in the proof of Theorem 1, we can write, assuming, without loss of generality, that node h is the node performing the update at the t-th iteration

$$\begin{aligned}
&y_h(t+1) = \\
&\quad = \lambda_h(t+1) - \lambda_h^* \\
&\quad = \left[\lambda_h(t) + \gamma\mathbf{1}_h^T\,(b\mathbf{1} - \hat{v}_G(t))\right]_+ - [\lambda_h^*]_+ \\
&\quad = \left[y_h(t) + \lambda_h^* + \gamma\mathbf{1}_h^T\,(b\mathbf{1} - \hat{v}_G(t))\right]_+ - [\lambda_h^*]_+ \\
&\quad = [y_h(t) + \lambda_h^* + \gamma\,(b_h - \hat{v}_h(q^*)) - \gamma\,(v_h(t) - \hat{v}_h(q^*))]_+ \\
&\qquad - [\lambda_h^*]_+
\end{aligned}$$

Let $\alpha_h = \lambda_h^* + \gamma\,(b_h - \hat{v}_h(q^*))$ and observe that $[\lambda_h^*]_+ = [\alpha_h]_+$. Hence we can write

$$\begin{aligned}
&y_h(t+1) = \\
&\quad = [y_h(t) + \alpha_h - \gamma\,(v_h(t) - \hat{v}_h(q^*))]_+ - [\alpha_h]_+ \\
&\quad = \left[y_h(t) + \alpha_h - \gamma\frac{2}{U_N^2}\sin\theta\mathbf{1}_h^T M\,(q(t) - q^*)\right]_+ - [\alpha_h]_+ \\
&\quad = \left[y_h(t) + \alpha_h - \gamma\frac{2}{U_N^2}\sin\theta\mathbf{1}_h^T Mx(t)\right]_+ - [\alpha_h]_+
\end{aligned}$$

where in the second equality we have used the fact that $v_h(t) - \hat{v}_h(q^*) = \frac{2}{U_N^2}\sin\theta\mathbf{1}_h^T M\,(q(t) - q^*)$.

As far as the variable x is concerned we have that

$$\begin{aligned}
&x_h(t+1) = \\
&\quad = q_h(t+1) - q_h^* \\
&\quad = q_h(t) + \sin\theta\lambda_h(t+1) - \mathbf{1}_h^T(q_G(t) + M^{-1}Nq_L) - q_h^* \\
&\quad = q_h(t) - q_h^* + \sin\theta\lambda_h(t+1) \\
&\qquad - \mathbf{1}_h^T(q_G(t) - q_G^* + q_G^* + M^{-1}Nq_L) \\
&\quad = x_h(t) + \sin\theta\lambda_h(t+1) - \mathbf{1}_h^T x(t) \\
&\qquad - \mathbf{1}_h^T(q_G^* + M^{-1}Nq_L) \\
&\quad = \sin\theta\lambda_h(t+1) - \mathbf{1}_h^T M^{-1}(Mq_G^* + Nq_L)
\end{aligned}$$

Now from (34a) we have that $\sin\theta\lambda_h^* = \mathbf{1}_h^T\left(q_G^* + M^{-1}Nq_L\right)$ and, in turn,

$$\begin{aligned}
x_h(t+1) &= \sin\theta\lambda_h(t+1) - \sin\theta\lambda_h^* \\
&= \sin\theta y_h(t+1)
\end{aligned}$$

Observe that Assumption 2 implies there exists almost surely a positive integer T such that any node has performed an update within the window $[0,T]$. It follows that, for $t \geq T$, $x(t) = \sin\theta y(t)$. Accordingly for $t \geq T$ the update for y can be rewritten as

$$y_h(t+1) = \left[y_h(t) + \alpha_h - \gamma\frac{2}{U_N^2}\sin^2\theta\mathbf{1}_h^T My(t)\right]_+ - [\alpha_h]_+$$

and, clearly, $y_k(t+1) = y_k(t)$, for $k \neq h$.

Now let $P_h = I - \gamma\frac{2}{U_N^2}\sin^2\theta\mathbf{1}_h\mathbf{1}_h^T M$. Using the fact that $\|a_+ - b_+\| \leq \|a-b\|$ it follows

$$\|y(t+1)\| \leq \|P_h y(t)\|.$$

Consider the evolution of the quantity $\mathbb{E}\left[\|y(t)\|^2\right]$. From the above inequality we get that

$$\begin{aligned}
\mathbb{E}\left[\|y(t+1)\|^2\right] &\leq \mathbb{E}\left[y(t)^T P_h^T P_h y(t)\right] \\
&= \text{trace}\mathbb{E}\left[y(t)^T P_h^T P_h y(t)\right] \\
&= \text{trace}\left\{\mathbb{E}\left[P_h^T P_h y(t)y(t)^T\right]\right\} \\
&\leq \left\|\mathbb{E}\left[P_h^T P_h\right]\right\| \text{ trace}\left\{\mathbb{E}\left[y(t)y(t)^T\right]\right\} \\
&\leq \left\|\mathbb{E}\left[P_h^T P_h\right]\right\| \mathbb{E}\left[\|y(t)\|^2\right] \qquad (35)
\end{aligned}$$

where, given two semidefinite matrices A, B, we used the fact that trace $\{AB\} \leq \|A\|$trace $\{B\}$. Let us compute $\mathbb{E}\left[P_h^T P_h\right]$. Observe that

$$\begin{aligned}
&P_h^T P_h = \\
&\quad = \left(I - \gamma\frac{2}{U_N^2}\sin^2\theta M\mathbf{1}_h\mathbf{1}_h^T\right)\left(I - \gamma\frac{2}{U_N^2}\sin^2\theta\mathbf{1}_h\mathbf{1}_h^T M\right) \\
&\quad = I - \gamma\frac{2}{U_N^2}\sin^2\theta(M\mathbf{1}_h\mathbf{1}_h^T + \mathbf{1}_h\mathbf{1}_h^T M) \\
&\qquad + \gamma^2\frac{4}{U_N^4}\sin^4\theta M\mathbf{1}_h\mathbf{1}_h^T M
\end{aligned}$$

from which we get, by using Assumption 2,

$$\begin{aligned}
\mathbb{E}\left[P_h^T P_h\right] &= \frac{1}{m-1}\sum P_h^T P_h \\
&= I - \gamma\frac{4}{U_N^2}\frac{\sin^2\theta}{m-1}M + \gamma^2\frac{4}{U_N^4}\frac{\sin^4\theta}{m-1}M^2.
\end{aligned}$$

By straightforward calculations one can see that the spectral radius of the above matrix is smaller than 1 if

$$\gamma < \frac{U_N^2}{\sin^2\theta\rho(M)}$$

where we recall that $\rho(M)$ denotes the spectral radius of M. Then, by Lemma 6, we have

$$\gamma < \frac{U_N^2}{\sin^2\theta(m-1)\max_h|Z_{0h}^{\text{eff}}|}. \qquad (36)$$

The proof can be concluded by invoking the Supermartingale Convergence Theorem [29]. For the sake of the clarity, we recall that this theorem states that, if X_t, $t \geq 0$, is a nonnegative random variable such that $\mathbb{E}[X_1] < +\infty$ and if $\mathbb{E}[X_{t+1}|\mathcal{F}_t] \leq X_t$ with probability one, where $\mathcal{F}_t$ denotes the history of the process X_t up to time t, then X_t tends to a limit X with probability one, and $\lim_{t\to\infty}\mathbb{E}[X_t] = \mathbb{E}[X]$.

Let $X_t = \|y(t)\|^2$. Observe that

$$\begin{aligned}
\mathbb{E}\left[\|y(t+1)\|^2 \,|\, y(t)\right] &\leq \mathbb{E}\left[y(t)^T P_h^T P_h y(t) \,|\, y(t)\right] \\
&\leq \left\|\mathbb{E}\left[P_h^T P_h\right]\right\| \; \|y(t)\|^2 \\
&\leq \|y(t)\|^2
\end{aligned}$$

where the last inequality follows from the fact that $\left\|\mathbb{E}\left[P_h^T P_h\right]\right\| < 1$ under condition (36). Moreover inequality (35) together with $\left\|\mathbb{E}\left[P_h^T P_h\right]\right\| < 1$ implies that $\lim_{t\to\infty}\mathbb{E}\left[\|y(t)\|^2\right] = 0$. Hence $\mathbb{E}\left[\|y(t)\|^2\right]$ converges with probability one to a nonnegative random variable X such that $\mathcal{E}[X] = 0$, i.e., X is the null random variable. This concludes the proof. ∎

References

[1] F. Katiraei and M. R. Iravani, "Power management strategies for a microgrid with multiple distributed generation units," *IEEE Trans. Power Syst.*, vol. 21, no. 4, pp. 1821–1831, Nov. 2006.

[2] M. Prodanovic, K. De Brabandere, J. Van den Keybus, T. Green, and J. Driesen, "Harmonic and reactive power compensation as ancillary services in inverter-based distributed generation," *IET Gener. Transm. Distrib.*, vol. 1, no. 3, pp. 432–438, 2007.

[3] B. Zhao, C. X. Guo, and Y. J. Cao, "A multiagent-based particle swarm optimization approach for optimal reactive power dispatch," *IEEE Trans. Power Syst.*, vol. 20, no. 2, pp. 1070–1078, May 2005.

[4] J. Lavaei, A. Rantzer, and S. H. Low, "Power flow optimization using positive quadratic programming," in *Proc. 18th IFAC World Congr.*, 2011.

[5] A. Y. S. Lam, B. Zhang, A. Dominiguez-Garcia, and D. Tse, "Optimal distributed voltage regulation in power distribution networks," *arXiv*, vol. [math.OC] 1204.5226, 2012.

[6] P. Tenti, A. Costabeber, P. Mattavelli, and D. Trombetti, "Distribution loss minimization by token ring control of power electronic interfaces in residential microgrids," *IEEE Trans. Ind. Electron.*, vol. 59, no. 10, pp. 3817–3826, Oct. 2012.

[7] S. Bolognani and S. Zampieri, "Distributed control for optimal reactive power compensation in smart microgrids," in *Proc. 50th IEEE Conf. on Decision and Control and European Control Conf. (CDC-ECC'11)*, Orlando, FL, Dec. 2011.

[8] W. H. Kersting, "Radial distribution test feeders," in *IEEE Power Engineering Society Winter Meeting*, vol. 2, Jan. 2001, pp. 908–912.

[9] J. A. Lopes, C. L. Moreira, and A. G. Madureira, "Defining control strategies for microgrids islanded operation," *IEEE Trans. Power Syst.*, vol. 21, no. 2, pp. 916–924, May 2006.

[10] T. C. Green and M. Prodanović, "Control of inverter-based micro-grids," *Electr. Pow. Syst. Res.*, vol. 77, no. 9, pp. 1204–1213, Jul. 2007.

[11] A. G. Phadke, "Synchronized phasor measurements in power systems," *IEEE Comput. Appl. Power*, vol. 6, no. 2, pp. 10–15, Apr. 1993.

[12] A. Costabeber, T. Erseghe, P. Tenti, S. Tomasin, and P. Mattavelli, "Optimization of micro-grid operation by dynamic grid mapping and token ring control," in *Proc. 14th European Conf. on Power Electronics and Applications (EPE)*, Birmingham, UK, 2011.

[13] J. Lavaei and S. H. Low, "Zero duality gap in optimal power flow problem," *IEEE Trans. Power Syst.*, 2011.

[14] D. P. Bertsekas, *Nonlinear programming*, 2nd ed. Belmont (MA): Athena Scientific, 1999.

[15] S. Bolognani and S. Zampieri, "A distributed control strategy for reactive power compensation in smart microgrids," *submitted to IEEE Transactions on Automatic Control*, 2012, arXiv preprint available [math.OC] 1106.5626.

[16] A. Ghosh, S. Boyd, and A. Saberi, "Minimizing effective resistance of a graph," *SIAM Rev.*, vol. 50, no. 1, pp. 37–66, Feb. 2008.

[17] A. Gómez-Expósito, A. J. Conejo, and C. Cañizares, *Electric energy systems. Analysis and operation*. CRC Press, 2009.

[18] H. Uzawa, *Studies in linear and nonlinear programming*. Stanford University Press, 1958, ch. The Kuhn-Tucker theorem in concave programming, pp. 32–37.

[19] R. D. Zimmerman, C. E. Murillo-Sánchez, and R. J. Thomas, "MATPOWER: steady-state operations, planning and analysis tools for power systems research and education," *IEEE Transactions on Power Systems*, vol. 26, no. 1, pp. 12–19, Feb. 2011.

[20] K. Turitsyn, P. Šulc, S. Backhaus, and M. Chertkov, "Options for control of reactive power by distributed photovoltaic generators," *Proc. IEEE*, vol. 99, no. 6, pp. 1063–1073, Jun. 2011.

[21] Y. G. Rebours, D. S. Kirschen, M. Trotignon, and S. Rossignol, "A survey of frequency and voltage control ancillary services - Part I: technical features," *IEEE Transactions on Power Systems*, vol. 22, no. 1, pp. 350–357, Feb. 2007.

[22] M. C. Chandorkar, D. M. Divan, and R. Adapa, "Control of parallel connected inverters in standalone AC supply systems," *IEEE Transactions on Industry Applications*, vol. 29, no. 1, pp. 136–143, Jan. 1993.

[23] K. De Brabandere, B. Bolsens, J. Van den Keybus, A. Woyte, J. Driesen, and R. Belmans, "A voltage and rrequency droop control method for parallel inverters," *IEEE Transactions on Power Electronics*, vol. 22, no. 4, pp. 1107–1115, Jul. 2007.

[24] E. Barklund, N. Pogaku, M. Prodanovic, C. Hernandez-Aramburo, and T. C. Green, "Energy management in autonomous microgrid using stability-constrained droop control of inverters," *IEEE Transactions on Power Electronics*, vol. 23, no. 5, pp. 2346–2352, Sep. 2008.

[25] J. Wang and N. Elia, "A control perspective for centralized and distributed convex optimization," in *Proceedings of the 50th IEEE Conference on Decision and Control (CDC)*, Orlando, FL (USA), Dec. 2011, pp. 3800–3805.

[26] S. Bolognani and S. Zampieri, "A distributed optimal control approach to dynamic reactive power compensation," in *Proc. 51st IEEE Conf. on Decision and Control (CDC)*, 2012.

[27] M. Ciobotaru, R. Teodorescu, P. Rodriguez, A. Timbus, and F. Blaabjerg, "Online grid impedance estimation for single-phase grid-connected systems using PQ variations," in *Proc. 38th IEEE Power Electronics Specialists Conf. (PESC)*, Jun. 2007.

[28] M. Ciobotaru, R. Teodorescu, and F. Blaabjerg, "On-line grid impedance estimation based on harmonic injection for grid-connected PV inverter," in *Proceedings of the IEEE International Symposium on Industrial Electronics (ISIE)*, 2007, pp. 2437–2442.

[29] L. Rogers and D. Williams, *Diffusions, Markov Processes and Martingales*, 2nd ed. Cambridge University Press, 1997.